RSC Advances

ROYAL SOCIETY OF CHEMISTRY

www.rsc.org/advances

Journal Name

ARTICLE

New Clathrates of $Rb_{7.50(1)}Tl_{0.50(1)}Ge_{46}$ and $K_{7.62(1)}Tl_{0.38(1)}Ge_{45.34(3)}$

Hui Zhang,[a,b,†] Gang Mu,[a,b] Fuqiang Huang[c,b] and Xiaoming Xie[a, b]

Received 00th January 20xx,
Accepted 00th January 20xx

DOI: 10.1039/x0xx00000x

www.rsc.org/

New Tl type-I clathrates of $K_{7.62(1)}Tl_{0.38(1)}Ge_{45.34(3)}$ and $Rb_{7.50(1)}Tl_{0.50(1)}Ge_{46}$ were synthesized via solid-state reaction. $Rb_{7.50(1)}Tl_{0.50(1)}Ge_{46}$ and $K_{7.62(1)}Tl_{0.38(1)}Ge_{45.34(3)}$ were found to crystallize in space group $Pm\bar{3}n$ and $Ia\bar{3}d$ with lattice parameter of a = 10.81559(7) Å and a = 21.4290(2) Å, respectively. Theoretical calculations indicated metallic features based on the calculation models of $Rb_7Tl_1Ge_{46}$ and $K_7Tl_1Ge_{46}$ in space group of $Pm\bar{3}$. The densities of states at Fermi level were predominantly determined by Ge s and Ge p orbits of $Rb_7Tl_1Ge_{46}$ and $K_7Tl_1Ge_{46}$.

Introduction

Clathrate compounds were comprised of host frameworks that embrace guest species in polyhedral cages. The first representatives were hydrates of various gases and liquids [1]. The discovery of sodium silicide Na_8Si_{46} and Na_xSi_{136} started the era of intermetallic and semiconducting clathrates [2-13]. Interest in clathrates had grown rapidly due to development of the "phonon glass–electron crystal" concept [14], according to which clathrates were promising thermoelectric materials. Further some clathrates demonstrated high thermoelectric figure of merit *ZT*, *e.g*. $Ba_8Ge_{30}Ga_{16}$ [15] with *ZT* = 1.3 at 800 K and $Ba_8Au_{5.3}Ge_{40.7}$ [16] with *ZT* = 0.92 at 600 K. Besides thermoelectric properties superconductivity and ferromagnetism were revealed for clathrates in $Ba_{8-x}Si_{46}$ [17], $Eu_8Ga_{16}Ge_{30}$ [18] and $Ba_8Mn_2Ge_{44}$ [19]. Binary, ternary and quaternary clathrates with various structure types have been synthesized [1-37]. To date type-I clathrates [1-2, 4-11, 14-17, 19-27], type-II clathrates [3, 12-13, 28-32], type-III clathrates [33-34], type-VIII clathrates [35-36], type-IX clathrates [18] and type-X clathrates [37] have been discovered.

The majority of clathrates belong to the type-I structure type, and most type-I clathrates crystallize in the cubic space group $Pm\bar{3}n$ [20-22]. The crystal structure feature a three-dimensional host framework, based on the group 14 elements Si, Ge and Sn, encapsulating guest atoms in large cavities. Strong covalent bonds exist within the framework, whereas the guest atoms are held within the framework cavities by weaker interactions. In polar clathrates electron balance between host and guest substructures obey the Zintl rules [38]. It implies that electronegative atoms accepted electrons from more electropositive atoms to complete the 8-electron shell.

The clathrates based on alkaline metal Si/Ge [2-8, 12-13] were synthesized previously by thermal decomposition the binary AM (A=alkali metal, M=Si/Ge) compounds. Later binary Tin based clathrates [9-11] and ternary clathrates [25-49] were prepared via solid-state reactions from the constituent elements. We have successfully prepared alkaline metal and thallium clathrate-II $Cs_8Na_{16-x}Tl_xGe_{136}$ via solid-state reaction [30]. Herein the synthesis and structure of thallium clathrate-I $Rb_{7.50(1)}Tl_{0.50(1)}Ge_{46}$ and $K_{7.62(1)}Tl_{0.38(1)}Ge_{45.34(3)}$ are reported.

Experimental

Synthetic procedure. The starting materials were high-purity elemental Rb, K, Tl and Ge. The assumed compositions of $Rb_6Tl_2Ge_{44}$ and $K_6Tl_2Ge_{44}$ was determined according to a clathrate-I containing 184 electrons per unit cell. Circa 1 gram of determined stoichiometric ratios of the mixed raw materials were loaded into Ta tubes. The containers were sealed by welding in an argon-filled glovebox [$c(O_2)$ and $c(H_2O)$ ≤ 1 ppm]. The Ta tubes were then taken out of the glovebox and put into quartz ampoules. The quartz tubes were sealed in a vacuum atmosphere, then heated at 650 °C for 2 weeks. The containers were then opened in air. The products were washed with distilled water and acetone then dried at 80 °C for 12h in air.

Morphology and Composition. The appropriately prepared metallographic specimens were investigated on a Philips XL 30 scanning electron microscope equipped with a LaB_6 cathode. The chemical composition was determined by energy dispersive X-ray spectroscopy (EDXS; EDXS Genesis Software V4.61) using a Si (Li) detector attached to the scanning electron microscope. Compositions were calculated from the background-corrected intensities of the X-ray lines Rb *L*, K *K*, Tl *L* and Ge *K*, which were excited by the electron beam at a 25 kV acceleration voltage. A standardless method with ZAF-matrix corrections was used.

[a] State Key Laboratory of Functional Materials for Informatics and Shanghai Center for Superconductivity, Shanghai Institute of Microsystem and Information Technology, Chinese Academy of Sciences, Shanghai 200050, China.
[b] CAS Center for Excellence in Superconducting Electronics, Shanghai 200050, China
[c] State Key Laboratory of High Performance Ceramics and Superfine Microstructures, Shanghai Institute of Ceramics, Chinese Academy of Sciences, Shanghai 200050, China.
† Email: huizhangmpg@hotmail.com.
Electronic Supplementary Information (ESI) available: CCDC-1430735 and 1430736. See DOI: 10.1039/x0xx00000x

Powder X-ray diffraction. The powder XRD patterns were collected using Guinier technique (Huber Image Plate Camera G670, Cu $K_{\alpha1}$ radiation, λ= 1.54056 Å, 3.0° < 2ϑ< 100.3°, step width 0.005°). The structures were resolved from powder XRD data by means of least-squares technique using the *WinCSD* program [50]. For structure presentation the program Diamond 3.0 was used [51].

Theoretical calculation. First-principle calculations were carried out by means of density functional theory using the pseudo-potential as implemented in the VASP code [52]. The exchange-correlation potential was calculated using the generalized gradient approximation (GGA) as proposed by Perdew Burke Ernzerhof [53]. The calculation accuracy was 10^{-5} eV using a 280 eV cut-off in the plane wave expansion and a 2*2*2 Monkhorst-Pack ***k*** grid on the simplified structure models of $Rb_7Tl_1Ge_{46}$ and $K_7Tl_1Ge_{45}$. $Rb_7Tl_1Ge_{46}$ structure model was obtained by first revision the crystallographic information file to get ordered file through changing the occupancy Tl1 to 1 to obtain $Rb_6Tl_2Ge_{46}$. Next the ordered model $Rb_6Tl_2Ge_{46}$ was input. Its symmetry was set to P1 then one Tl1 atom was changed to Rb1. A new symmetry of $Pm\bar{3}$ was found and the calculation model $Rb_7Tl_1Ge_{46}$ in $Pm\bar{3}$ was obtained. $K_{7.62(1)}Tl_{0.38(1)}Ge_{45.34(3)}$ in space group of $Ia\bar{3}d$ was a 2*2*2 times superstructure of $Rb_{7.50(1)}Tl_{0.50(1)}Ge_{46}$. For simplicity we used crystallographic information file of $Rb_{7.50(1)}Tl_{0.50(1)}Ge_{46}$ as the original model of $K_{7.62(1)}Tl_{0.38(1)}Ge_{45.34(3)}$ by changing the lattice parameter to 10.7145(1) Å in space group $Pm\bar{3}n$, setting Rb1 and Rb2 to Tl1 and K2 with complete occupancy to obtain ordered $K_6Tl_2Ge_{46}$. $K_6Tl_2Ge_{46}$ was imported. Its symmetry was set to P1, then one Tl1 was changed to K1. A new symmetry of $Pm\bar{3}$ was found and the calculation model of $K_7Tl_1Ge_{46}$ was obtained. The ordered input files of $Rb_6Tl_2Ge_{46}$ and $K_6Tl_2Ge_{46}$ together with the calculation models of $Rb_7Tl_1Ge_{46}$ and $K_7Tl_1Ge_{46}$ as well as their structure figures were given as supplementary materials.

Results and discussion

Morphology and composition. The synthesized samples of $Rb_{7.50(1)}Tl_{0.50(1)}Ge_{46}$ (inset of Figure 1 top) and $K_{7.62(1)}Tl_{0.38(1)}Ge_{45.34(3)}$ (inset of Figure 1 bottom) samples were grey particles of 100-200 μm and had distinct facets. The elemental compositions were confirmed by EDX analysis as $K_{7.6(5)}Tl_{1.5(1)}Ge_{45.0(4)}$ and $Rb_{7.0(2)}Tl_{1.7(5)}Ge_{45.03(8)}$ with large standard errors. The final compositions of $K_{7.62(1)}Tl_{0.38(1)}Ge_{45.34(3)}$ and $Rb_{7.50(1)}Tl_{0.50(1)}Ge_{46}$ were determined by structural refinement based on powder XRD data.

X-ray powder diffraction. The peak searching, indexing and structural refinement were performed on powder XRD data using *WinCSD* software [50]. The indexed X-ray powder diffraction data indicated $Rb_{7.50(1)}Tl_{0.50(1)}Ge_{46}$ was a type-I clathrate in space group $Pm\bar{3}n$ with unit cell parameter of *a* = 10.81559(7) Å and Ge impurity was observed. $K_{7.62(1)}Tl_{0.38(1)}Ge_{45.34(3)}$ was indexed using a 2*2*2 times superstructure in space group $Ia\bar{3}d$ with lattice parameters of *a* = 21.4290(2) Å.

Structure refinement. The full profile simulated X-ray powder diffraction patterns of $Rb_{7.50(1)}Tl_{0.50(1)}Ge_{46}$ (top) and $K_{7.62(1)}Tl_{0.38(1)}Ge_{45.34(3)}$ (bottom) were given in Figure 1 with experimental data in red circles, simulated curves in black lines, brag sites in black bars and difference curves in black lines. Weak impurity peaks appeared in $Rb_{7.50(1)}Tl_{0.50(1)}Ge_{46}$ (top) and $K_{7.62(1)}Tl_{0.38(1)}Ge_{45.34(3)}$ (bottom), which belonged to Tl rich mixtures in Tl-Ge-Rb/K system according to SEM images and EDX analysis.

The structures of $Rb_{7.50(1)}Tl_{0.50(1)}Ge_{46}$ and $K_{7.62(1)}Tl_{0.38(1)}Ge_{45.34(3)}$ were resolved by direct method using the *WinCSD* program. During the refinement procedures for $Rb_{7.50(1)}Tl_{0.50(1)}Ge_{46}$ the three framework atom sites of 6*c*, 16*i*, and 24*k* were set as Ge1, Ge2 and Ge3, the guest atom sites at the 2*a* and 6*d* sites were set as Rb1 and Rb2 in a typical clathrate-I structure. The displace parameter for Rb1 (at 2*a*) was found too low. The subsequent refined occupancy indicated possible heavier atom in this site. Finally Rb1 was refined with Tl1 together. The structure refinement yielded complete occupancies for Ge1, Ge2, Ge3 and Rb2 in $Rb_{7.50(1)}Tl_{0.50(1)}Ge_{46}$.

$K_{7.62(1)}Tl_{0.38(1)}Ge_{45.34(3)}$ crystallized in a 2*2*2 times superstructure in $Ia\bar{3}d$ space group. During the refinement procedures for $K_{7.62(1)}Tl_{0.38(1)}Ge_{45.34(3)}$ the six framework atom sites of 24c, 24d, 32e and three *96h* were set as Ge1, Ge2, Ge3, Ge4, Ge5 and Ge6, the guest atom sites at the 16*a* and 48*g* sites were set as K1 and K2.The displacement parameter for K1 was found too low. The refined occupancy indicated possible heavier atom in this position. Subsequently K1 site was refined with Tl1. The displacement parameters for Ge1 (at 24*c*) and Ge2 (at 24*d*) were higher than that of other Ge sites. The subsequent refinement indicated partial vacancies at Ge1 and Ge2 sites. The refinement yielded complete occupancies for Ge3, Ge4, Ge5, Ge6 and K2.

The final atomic coordinates, site occupancies, isotropic atomic displacement parameters and *R* factors for $Rb_{7.50(1)}Tl_{0.50(1)}Ge_{46}$ and $K_{7.62(1)}Tl_{0.38(1)}Ge_{45.34(3)}$ were listed in Table 1. The selected bond distances and angles of $Rb_{7.50(1)}Tl_{0.50(1)}Ge_{46}$ and $K_{7.62(1)}Tl_{0.38(1)}Ge_{45.34(3)}$ were given in Table 2 as supplemental materials.

Structure description. The crystal structures of $Rb_{7.50(1)}Tl_{0.50(1)}Ge_{46}$ (left) and $K_{7.62(1)}Tl_{0.38(1)}Ge_{45.34(3)}$ (right) were shown in Figure 2. $Rb_{7.50(1)}Tl_{0.50(1)}Ge_{46}$ crystallized in a type-I clathrate structure in space group $Pm\bar{3}n$. The clathrate-I contains 46 framework Ge atoms which form two kinds of polyhedral cages. One kind of yellow pentagonal dodecahedron was composed of 12 pentagonal faces ($[5^{12}]$) formed by 8 Ge2 (cyan, at 16*i* site) and 12 Ge3 (blue, at 24*k* site). Another kind of violet tetrakaidecahedron was built of 2 hexagonal and 12 pentagonal faces ($[5^{12}6^2]$) formed by 4 Ge1 (brown, at 6*c* site), 8 Ge2 and 12 Ge3. The violet tetrakaidecahedra formed the fused the perpendicular double chains in the middle of a couple of opposite edges of three directions in the unit cell by sharing the hexagonal faces. The yellow pentagonal dodecahedra shared 12 pentagonal faces with 12 tetrakaidecahedra, filled the rest vacancies of the corners and body center of the cubic lattice. Red Rb1 (at 2*a* site) lied in the center of the cage of yellow pentagonal dodecahedron. Violet Rb2 (at 6*d* site) located in the violet tetrakaidecahedron center.

$K_{7.62(1)}Tl_{0.38(1)}Ge_{45.34(3)}$ crystallized $Ia\bar{3}d$ space group with 2*2*2 times superstructure of clathrate-I. Wyckoff site transformation from $Pm\bar{3}n$ space group to $Ia\bar{3}d$ space group was shown in scheme I. In $K_{7.62(1)}Tl_{0.38(1)}Ge_{45.34(3)}$ superstructure K1/Tl1 (red at 16*a*) and K2(violet at 48*g*) were deduced from 2*a* and 6*d*; Ge1(brown at 24*c*)/Ge2(yellow at 24*d*), Ge3(green at 32*e*)/Ge4(cyan at 96*h*) and Ge5(blue at 96*h*)/Ge6(deep blue at

96*h*) were split from 6*c*, 16*i* and 24*k* sites in $Pm\bar{3}n$. The structure of $K_{7.62(1)}Tl_{0.38(1)}Ge_{45.34(3)}$ was isotypic with Ba_8Ge_{43} ($Ia\bar{3}d$) [24]. In Ba_8Ge_{43} Ge preferred at 24*d* sites and vacancies preferred at 24c sites. Ba2 deviated less from the center of tetrakaidecahedron compared with K2. In $Rb_{7.50(1)}Tl_{0.50(1)}Ge_{46}$, Rb1/Tl1—Ge2/Ge3 distances in dodecahedron varied in a small range of 3.4360(9) to 3.563(1) Å and Rb2—Ge distances in tetrakaidecahedron changed in a large range of 3.6514 (8) to 4.162(1) Å. Ge—Ge bond distances altered in the range of 2.4902(7) to 2.584 (2) Å. Ge1—Ge3—Ge3 bond angle 124.09(5)° in the six member ring deviated furthest from ideal tetrahedral angle of 109°08' compared with others.

In $K_{7.62(1)}Tl_{0.38(1)}Ge_{45.34(3)}$, K1/Tl1—Ge2/Ge3 distances in dodecahedron varied in a small range of 3.357(3) to 3.636(3) Å. K2—Ge1/Ge2/Ge3 distances in tetrakaidecahedron changed in a large range of 3.359(4) to 4.387(5) Å. The shortest Ge3-Ge3 bond length was 2.237(4) Å and the longest Ge4-Ge4 bond length was 2.600(4) Å. Ge1—Ge5—Ge6 bond angle 126.83(14)° and Ge2—Ge6—Ge5 bond angle 122.27(5)° in six-member ring deviated far away from an ideal tetrahedral angle of 109°08' compared with others.

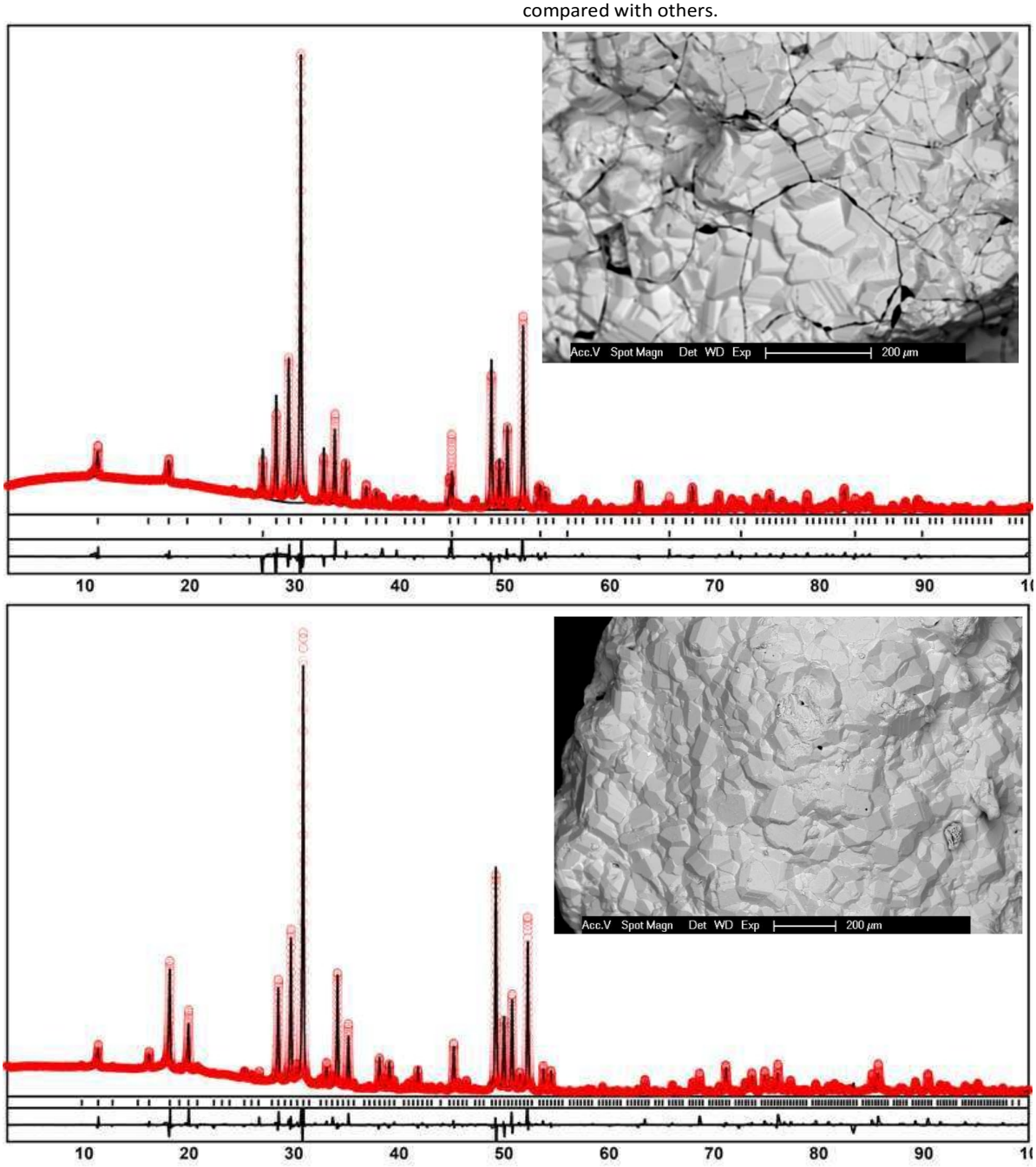

Figure 1. Full profile simulated XRD patterns of $Rb_{7.50(1)}Tl_{0.50(1)}Ge_{46}$ (refined with Ge impurity) (top) and $K_{7.62(1)}Tl_{0.38(1)}Ge_{45.34(3)}$ (bottom), inset of which are their corresponding SEM images.

Journal Name

ARTICLE

Table 1. Atomic coordinates and equivalent isotropic displacement parameters (Å^2) for $Rb_{7.50(1)}Tl_{0.50(1)}Ge_{46}$ and $K_{7.62(1)}Tl_{0.38(1)}Ge_{45.34(3)}$.

Atom	site	x	y	z	*Uiso*	*Occ.*
$Rb_{7.50(1)}Tl_{0.50(1)}Ge_{46}$		a = 10.81559(7) Å	R=9.33	$Pm\bar{3}n$		
Rb1/Tl1	2a	0	0	0	0.00319(3)	0.750(4)/0.250(4)
Rb2	6d	1/4	0	1/2	0.02164(3)	1
Ge1	6c	1/4	1/2	0	0.00354(3)	1
Ge2	16i	0.18341(8)	x	x	0.01537(3)	1
Ge3	24k	0	0.1194(1)	0.3070 (1)	0.01988(3)	1
$K_{7.62(1)}Tl_{0.38(1)}Ge_{45.34(3)}$		a =21.4290(2) Å	R=11.4	$Ia\bar{3}d$		
K1/Tl1	16a	0	0	0	0.02774(8)	0.810(6)/0.190(6)
K2	48g	1/8	0.2380(2)	0.0119(2)	0.00859(8)	1
Ge1	24c	1/8	0	1/4	0.01592(8)	0.90(1)
Ge2	24d	3/8	0	1/4	0.02788(8)	0.88(1)
Ge3	32e	0.0948(2)	0.0948(2)	0.0948(2)	0.01742(8)	1
Ge4	96h	0.1569(2)	0.3445(2)	0.1667(1)	0.01051(8)	1
Ge5	96h	0.0914(1)	0.2512(2)	0.1899(2)	0.00938(8)	1
Ge6	96h	0.0948(1)	0.2432(2)	0.3103(2)	0.00740(8)	1

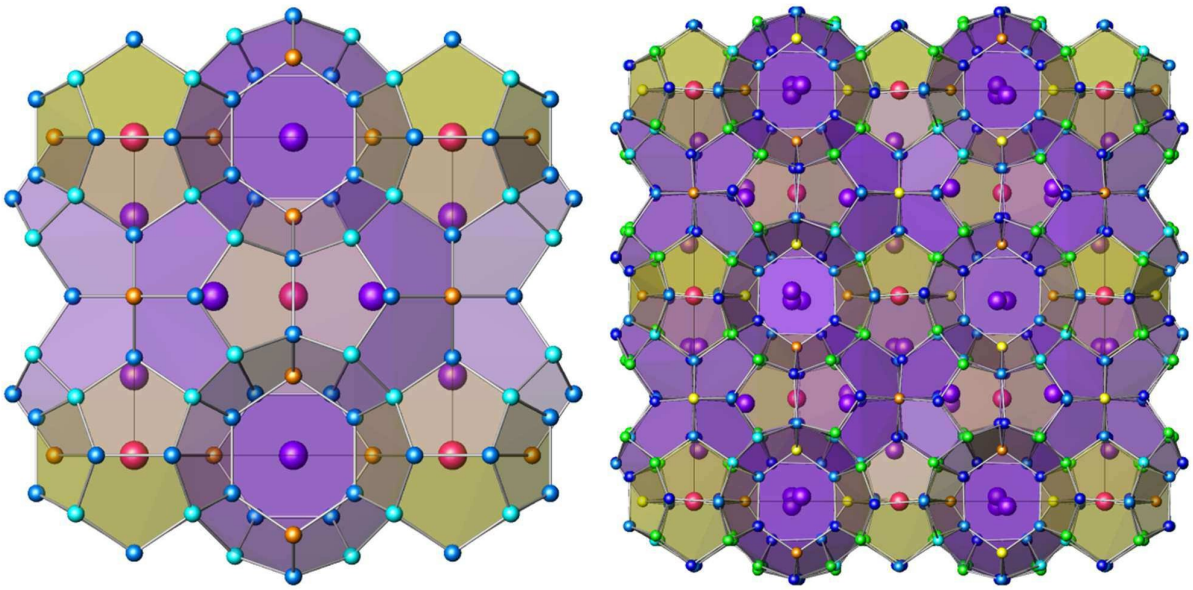

Figure 2. Clathrate-I structure of $Rb_{7.50(1)}Tl_{0.50(1)}Ge_{46}$ (left): brown Ge1 at 6*c* sites, cyan Ge2 at 16*i* and blue Ge3 at 24*k* sites form the violet tetrakaidecahedron caged with violet Rb2 (at 6*d*); Ge2 and Ge3 construct yellow pentagonal dodecahedron caged with red Rb1/Tl1 (at 2*a*). The 2*2*2 times superstructure of clathrate-I of $K_{7.62(1)}Tl_{0.38(1)}Ge_{45.34(3)}$ (right) with partial ordering of vacancies brown Ge1 (at 16*a*) and yellow Ge2 (at 48*g*), green Ge3 (at 32*e*), cyan Ge4 (at 96*h*), blue Ge5 (at 96*h*), deep blue Ge6 (at 96*h*) form the violet tetrakaidecahedron caged with violet Rb2 (at 48*g*) which deviates from the center of tetrakaidecahedron; Ge3, Ge4, Ge5 and Ge6 construct yellow pentagonal dodecahedron caged with red K1 (at 16*a*).

Journal Name

ARTICLE

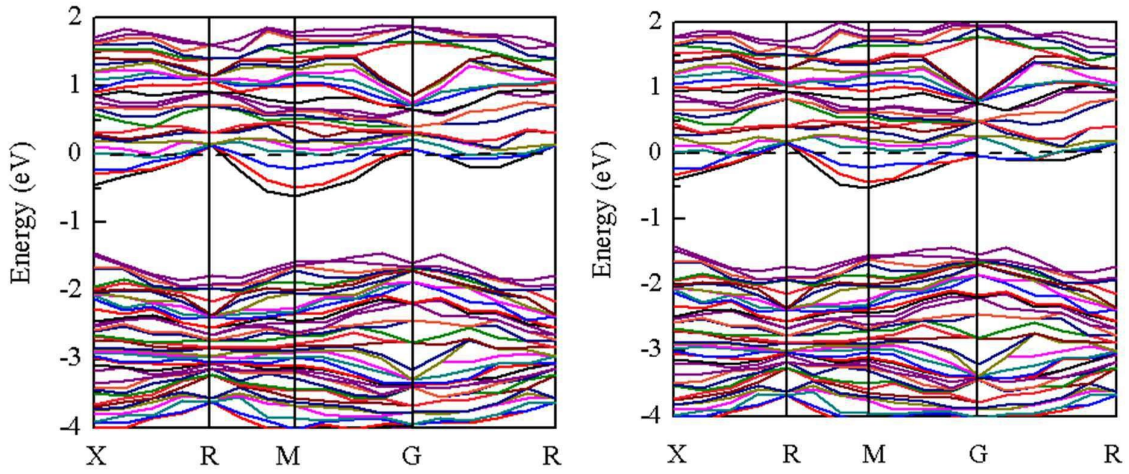

Figure 3. The band structures of $Rb_7Tl_1Ge_{46}$ (left) and $K_7Tl_1Ge_{46}$ (right)

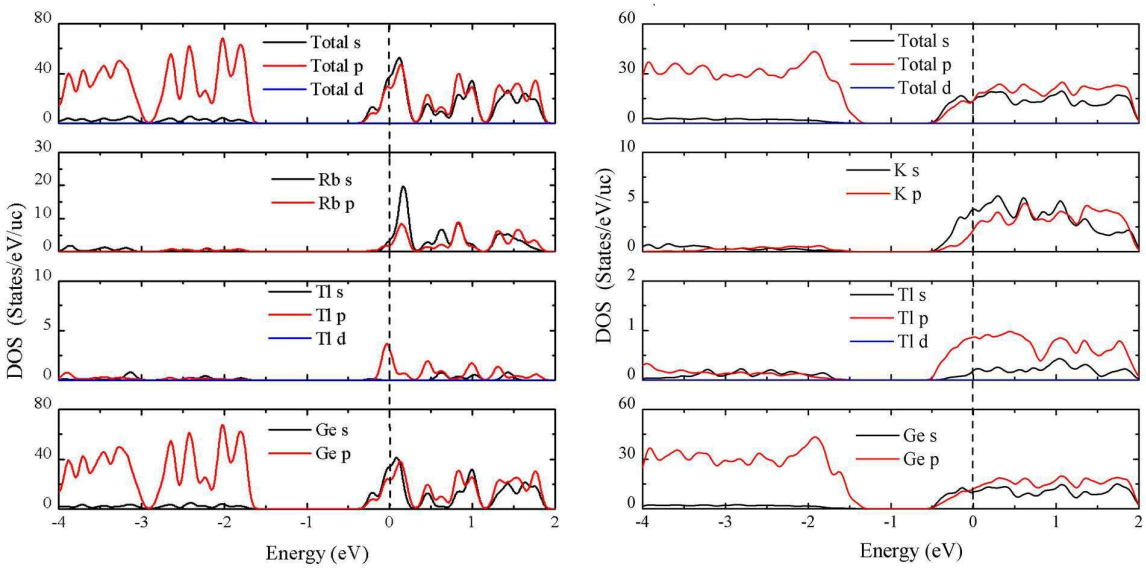

Figure 4. Total and atom deduced densities of states of $Rb_7Tl_1Ge_{46}$ (left) and $K_7Tl_1Ge_{46}$ (right).

atom	color	$Pm\bar{3}n$	→	$Ia\bar{3}d$	atom	color
Rb1/Tl1	red	2*a*	→	16*a*	K1/Tl1	red
Rb2	violet	6*d*	→	48*g*	K2	violet
Ge1	brown	6*c*	↗	24*c*	Ge1	brown
			↘	24*d*	Ge2	yellow
Ge2	cyan	16*i*	↗	32*e*	Ge3	green
			↘	96*h*	Ge4	cyan
Ge3	blue	24*k*	↗	96*h*	Ge5	blue
			↘	96*h*	Ge6	deep blue

Scheme I Wyckoff sites occupied in the transformation from space group $Pm\bar{3}n$ to space group $Ia\bar{3}d$.

Theoretical calculation. Theoretical calculations were performed based on simplified models of $Rb_7Tl_1Ge_{46}$ and $K_7Tl_1Ge_{46}$ in $Pm\bar{3}$ space group as described in theoretical calculations section. Calculated band structures and high-symmetry axes of the Brillouin Zone for $Rb_7Tl_1Ge_{46}$ and $K_7Tl_1Ge_{46}$ models are shown in Figure 3. The abscissa in Figure 3 indicate the high symmetry directions in Brillouin zone paths of X(0.5, 0, 0), R(0.5, 0.5, 0.5), M(0.5, 0.5, 0) and G(0, 0, 0) in the reciprocal lattices of $Rb_7Tl_1Ge_{46}$ and $K_7Tl_1Ge_{46}$. The dashed lines correspond to Fermi energy level. The other coloured lines of

the figures are electronic energy levels of different bands, which are occupied by electrons below Fermi energy level and are empty above Fermi level. The band structures indicate metallic features for $Rb_7Tl_1Ge_{46}$ and $K_7Tl_1Ge_{46}$. The atom deduced densities of States (DOS) for $Rb_7Tl_1Ge_{46}$ and $K_7Tl_1Ge_{46}$ are given in Figure 4. DOS at Fermi level are mainly determined by Ge s, Ge *p* orbits, partial Tl *p* orbits and Rb *s* and Rb *p* or K *s*, K *p* in $Rb_7Tl_1Ge_{46}$ and $K_7Tl_1Ge_{46}$.

Conclusions

Type-I clathrates of $Rb_{7.50(1)}Tl_{0.50(1)}Ge_{46}$ and $K_{7.62(1)}Tl_{0.38(1)}Ge_{45.34(3)}$ were synthesized from constituent elements. $Rb_{7.50(1)}Tl_{0.50(1)}Ge_{46}$ crystallized in a clathrate-I structure in $Pm\bar{3}n$ space group with the unit cell parameter of *a* = 10.81559(7)Å. $K_{7.62(1)}Tl_{0.38(1)}Ge_{45.34(3)}$ was a 2*2*2 times superstructure of clathrate-I, which crystallized in $Ia\bar{3}d$ space group with lattice parameter of *a* = 21.4290(2) Å. The structural transformation from $Rb_{7.50(1)}Tl_{0.50(1)}Ge_{46}$ in $Pm\bar{3}n$ to $K_{7.62(1)}Tl_{0.38(1)}Ge_{45.34(3)}$ in $Ia\bar{3}d$ was indicated. The band structures indicated metallic features for both $Rb_7Tl_1Ge_{46}$ and $K_7Tl_1Ge_{46}$. The densities of states at Fermi level were mainly determined by Ge *s* and Ge *p* orbits in $Rb_7Tl_1Ge_{46}$ and $K_7Tl_1Ge_{46}$.

Acknowledgements

This work was financially supported by the Strategic Priority Research Program (B) of the Chinese Academy of Sciences (Grants XDB04040200 andXDB04040300).

Notes and references

1 (a) G. A. Jeffrey, in Inclusion Compounds, Eds. J. L. Atwood, J. E.D. Davies, D. D. MacNicol, Academic Press Inc., London, UK, 1984.(b) E. D. SloanJr., Clathrate hydrates of natural gases, 2nd ed.; Marcel Dekker Inc.: New York, 1998.

2 (a) C. Cros, M. Pouchard, P. Hagenmuller, J. Solid State Chem. 1970, **2**, 570-58. (b) J. S. Kasper, P. Hagenmuller, M. Pouchard, C.Cros, *Science*, 1965, **150**, 1713–1714. (c) C. Cros, M. Pouchard, P. Hagenmuller, *Bull. Soc. Chim. France*, 1971, **1971**, 379–386. (d) C. Cros, J.-C. Benejat, *Bull. Soc. Chim. France* 1972, **1972**, 1739–1743. (e) M. Beekman, C. P. Sebastian, Yu. Grin, G. S. Nolas, *J. Electr. Mater.* 2009, **38**, 1136–1141. (f) H. O. Horie, T. Kikudome, K. Teramura, S. Yamanaka, *J. Solid State Chem.* 2009, **182**, 129–135. (g) M. Beekman, E. N. Nenghabi, K. Biswas, C. W. Myles, M. Baitinger, Yu. Grin, G. S. Nolas, *Inorg. Chem*. 2010, **49**, 5338–5340.

3 (a) E. Reny, P. Gravereau, C. Cros, M. Pouchard, *J. Mater. Chem.* 1998, **8**, 2839–2844. (b) G. K. Ramachandran, J. Dong, J. Diefenbacher, J. Gryko, R. F. Marzke, O. F. Sankey, P. F. McMilan, *J. Solid State Chem*. 1999, **145**, 716–730. (c) M. Beckman, M. Baitinger, H. Borrmann, W. Schnelle, K. Meier, G. S. Nolas, Yu. Grin, J. Am. Chem. Soc. 2009, **131,** 9642-9643.

4 (a) J. Gallmeier, H. Schaefer, A. Weiss, *Z. Naturforsch.* 1967, **22B**, 1080–1080. (b) G. K. Ramachandran, P. F. McMillan, J. Dong, O. F. Sankey, *J. Solid State Chem.* 2000, **154**, 626–634. (c) C. Cros, M. Pouchard, P. Hagenmuller, J. S. Kasper, *Bull. Soc. Chim. France*, 1968, **1968**, 2737–2742. (d) B. Boehme, A. M. Guloy, Z. Tang, W. Schnelle, U. Burkhardt, M. Baitinger, Yu. Grin, *J. Am. Chem. Soc.* 2007, **129**, 5348–5349.

5 A. Wosylus, I. Veremchuk, W. Schnelle, M. Baitinger, U. Schwarz, Yu. Grin, *Chem Euro. J.* 2009, **15**, 5901–5903.

6 (a) J. Gallmeier, H. Schaefer, A. Weiss, *Z. Naturforsch.* 1969, **24B**, 665-667. (b) H. G. von Schnering, J. Llanos, K. Peters, M. Baitinger, Yu. Grin, R. Nesper, *Z. Kristallogr.-NCS.* 2011,**226**, 9–10.

7 F. Dubois, T. F. Faessler, J. Am. Chem. Soc. 2005,127, 3264–3265

8 A. Kaltzoglou, T. Faessler, M. Christensen, S. Johnsen, B. Iversen, I. Presniakov, A. Sobolev, A. Shevelkov, *J. Mater. Chem.* 2008, **18**, 5630–5637.

9 (a) H. G. von Schnering, R. Kroener, M. Baitinger, K. Peters, R. Nesper, Yu. Grin, *Z. Kristallogr. NCS.* 2000, **215**, 205–206. (b) A. Kaltzoglou, S. D. Hoffmann, T. F. Faessler, *Euro. J. Inorg. Chem.*2007, **26**, 4162–4167.

10 (a) Yu. Grin, L. Z. Melekhov, K. A. Chuntonov, S. P. Yatsenko, *Sov. Phys. Crystallog.* 1987, **32**, 290–291. (b) L. Z. Melekhov, S. P. Yatsenko, K. A. Chuntonov, Y. N. Grin, *Russ. Metall.* 1987, **2**, 208–211.

11 I. Veremchuk, A. Wosylus, B. Boehme, M. Baitinger, H. Borrmann, Yu. Prots, U. Burkhardt, U. Schwarz, Yu. Grin, *Z. Anorg. Allg. Chem.*2011, **637**, 1281–1286.

12 S. Stefanoski, G. S. Nolas, *Crystal Growth and Design*, 2011, **11**, 4533–4537.

13 A. M. Guloy, Z. Tang, R. Ramlau, B. Boehme, M. Baitinger, Yu. Grin, *Euro. J. Inorg. Chem.* 2009, **17**, 2455–2458.

14 G. A. Slack, in CRC Handbook of thermoelectrics, Ed. D. M. Rowe, Chemical Rubber: Boca Raton, FL, 1995, **2**, 407.

15 (a) G. S. Nolas, J. L. Cohn, G. A. Slack, S. B. Schujman, *Appl. Phys. Lett.* 1998, **73**, 178–180. (b) A. Saramat, G. Svensson, A. E. C. Palmqvist, C. Stiewe, E. Mueller, D. Platzek, S. G. K. Williams, D. M. Rowe, J. D. Bryan, G. D. Stucky, *J. Appl. Phys*. 2006, **99**, 023708.

16 H. Zhang, H. Borrmann, N. Oeschler, C. Candolfi, W. Schnelle, M. Schmidt, U. Burkhardt, M. Baitinger, J. T. Zhao, Yu. Grin, *Inorg. Chem.* 2011, **50**, 1250–1257.

17 (a) S. Yamanaka, E. Enishi, H. Fukuoka, M. Yasukawa, *Inorg. Chem.* 2000, **39**, 56−58. (b) H. Fukuoka, J. Kiyoto, S. J. Yamanaka, *Solid State Chem.* 2003, **175**, 237−244. (c) H. Fukuoka, J. Kiyoto, S. J. Yamanaka, *Inorg. Chem.* 2003, **42**, 2933−2937. (d) H. Fukuoka, J. Kiyoto, S. Yamanaka, *J. Phys. Chem. Solid,* 2004, **65**, 333−336.

18 S. Paschen, W. Carrillo-Cabrera, A. Bentien, V. H. Tran, M. Baenitz, Yu. Grin, F. Steglich, *Phys. Rev. B* 1999, **64**, 214404.

19 T. Kawaguchi, K. Tanigaki, M. Yasukawa, *Appl. Phys. Lett.* 2000, **77**, 3438−3440.

20 A. V. Shevelkov, K. A. Kovnir, *Struct. Bonding* (Berlin) **139**, 2011, 97−144.

21 M. A. Kirsanova, A. V. Olenev, A. M. Abakumov, M. A. Bykov, A. V. Shevelkov, *Angew. Chem., Int. Ed*. 2011, **50**, 2371−2374.

22 K. A. Kovnir, A. V. Shevelkov, *Russ. Chem. Rev.* 2004, **73**, 923–938.

23 K. Kovnir, U. Stockert, S. Budnyk, Y. Prots, M. Baitinger, S. Paschen, A. V. Shevelkov, Yu. Grin, *Inorg. Chem*. 2011, **50**, 10387–10396.

24 (a) F. Dubois, T. F. Faessler, *Z. Anorg. Allg. Chem*. 2004, **630**, 1718–1718. (b) W. Carrillo-Cabrera, S. Budnyk, Yu. Prots, Yu. Grin, *Z. Anorg. Allg. Chem*. 2004, **630**, 2267–2276. (c) N. L. Okamoto, K. Tanaka, H. Inui, *Acta Mater.* 2006, **54**, 173–178. (d) U. Aydemir, C. Candolfi, H. Borrmann, M. Baitinger, A. Ormeci, W. Carrillo-Cabrera, C. Chubilleau, B. Lenoir, A. Dauscher, N. Oeschler, F. Steglich, Yu. Grin, *Dalton Trans.* 2010, **39**, 1078–1088.

25 W. Jung, J. Loeincz, R. Ramlau, H. Borrmann, Y. Prots, F. Haarmann, W. Schnelle, U. Burkhardt, M. Baitinger, Yu. Grin, *Angew. Chem., Int. Ed.* 2007, **46**, 6725–6728.
26 (a) H. Zhang, M. Baitinger, L. Fang, W. Schnelle, H. Borrmann, U. Burkhardt, A. Ormeci, J. T. Zhao, Yu. Grin, *Inorg. Chem.* 2013, **52**, 9720–9726. (b) H. Zhang, X. Xu, W.Li, G. Mu, F. Huang, X. Xie, *RSC Adv.* 2015, **5**, 53829.
27 H. G. von Schnering, R. Kroener, H. Menke, K. Peters and R. Nesper, *Z. Kristallogr. NCS.* 1998, **213**, 677-678.
28 (a) S. Bobev, S. C. Sevov, J. Am. Chem. Soc. 1999,**121**, 3795–3796. (b) S. Bobev, S. C. Sevov, J. Solid State Chem. 2000, **153**, 92-105.
29 A. M. Guloy, R. Ramlau, Z. Tang, W. Schnelle, M. Baitinger, Yu. Grin, *Nature*, 2006,**443**, 320–323.
30 M. Beekman, G. S. Nolas, J. Mater. Chem. 2008, **18**, 842–851.
31 M. K. Beekman, Synthesis and Characterization of Type II Silicon and Germanium Clathrates, Graduate Theses and Dissertations (2006). http: //scholarcommons.usf.edu/etd/3865.
32 H. Zhang, X. Xu, W. Li, G. Mu, F. Huang, X. Xie, Dalton Trans. 2015, **44**, 16937–16945.
33 J. V. Zaikina, W. Schnelle, K. A. Kovnir, A. V. Olenev, Yu. Grin, A. V. Shevelkov, *Solid State Sci.* 2007, **9**, 664–671.
34 J. V. Zaikina, K. A. Kovnir, F. Haarmann, W. Schnelle, U. Burkhardt, H. Borrmann, U. Schwarz, Yu. Grin, A. V. Shevelkov, *Chem. Eur. J.* 2008, **14**, 5414–5422.
35 J. T. Zhao, J. D. Corbett, *Inorg. Chem.* 1994, **33**, 5721–5726.
36 (a) H. Fukuoka, K. Iwai, S. Yamanaka, H. Abe, K. Yoza, L. Haeming, *J. Solid State Chem.* 2000, **151**, 117–121. (b) S. J. Kim, S. Hu, C. Uher, T. Hogan, B. Huang, J. D. Corbett, M. G. Kanatzidis, *J. Solid State Chem.* 2000, **153**, 321–329.(c) W. Carrillo-Cabrera, J. Curda, H. G. von Schnering, S. Paschen, Yu. Grin, *Z. Kristallogr. NCS,* 2000, **215**, 207–208. (d) J. H. Kim, N. L. Okamoto, K. Kishida, K. Tanaka, H. Inui, *J. Appl. Phys.* 2007, **102,** 094506. (e) W. Carrillo-Cabrera, H. Borrmann, S. Paschen, M. Baenitz, F. Steglich, Yu. Grin, *J. Solid State Chem*. 2005, **178**, 715–728.
37 M. A. Kirsanova, A. V. Olenev, A. M. Abakumov, M. A. Bykov, A. V. Shevelkov, Angew. Chem. Inter. Ed. 2011, **50**, 2371–2374.
38 Ed. M. S. Kauzlarich, Chemistry, Structure and Bonding of Zintl Phases and Ions, VCH Publishers: New York, NY, 1996.
39 (a) H. G. von Schnering, H. Menke, Angew. Chem., Int. Ed. 1972, **11**, 43–44. (b) H. Menke, H. G. von Schnering, *Naturwissenschaften* 1972, **59**, 420–420. (c) H. G. von Schnering, H. Menke, Z. Anorg. Allg. Chem. 1976, **424**, 108–114. (d) H. Menke, H. G. von Schnering, Z. Anorg. Allg. Chem. 1973, **395**, 223–238.
40 (a) M. M. Shatruk, K. A. Kovnir, A. V. Shevelkov, I. A. Presniakov, B. A. Popovkin, *Inorg. Chem.* 1999, **38**, 3455−3457. (b) K. A. Kovnir, M. M. Shatruk, L. N. Reshetova, I. A. Presniakov, E. V. Dikarev, M. Baitinger, F. Haarmann, W. Schnelle, M. Baenitz, Y. Grin, A. V. Shevelkov, *Solid State Sci.* 2005, **7**, 957−968. (c) K. A. Kovnir, A. V. Sobolev, I. A. Presniakov, O. I. Lebedev, G. Van Tendeloo, W. Schnelle, Y. Grin, A. V. Shevelkov, *Inorg. Chem.* 2005, **44**, 8786−8793. (d) K. Kishimoto, S. Arimura, T. Koyanagi, *Appl. Phys. Lett.* 2006, **88**, 222115.
41 (a) K. A. Kovnir, A. N. Uglov,J. V. Zaikina, A. V. Shevelkov, *Mendeleev Commun*. 2004, **4**, 135−136. (b) E. Reny, S. Yamanaka, C. Cros, M. Pouchard, *Chem. Commun.* 2000, 2505−2506.
42 J. V. Zaikina, K. A. Kovnir, A. V. Sobolev, I. A. Presniakov, Yu. Prots, M. Baitinger, W. Schnelle, A. V. Olenev, O. I. Lebedev, G. van Tendeloo, Yu. Grin, A. V. Shevelkov, *Chem. Eur. J*. 2007, **13**, 5090–5099.
43 M. M. Shatruk, K. A. Kovnir, M. Lindsjo, I. A. Presniakov, L. A. Kloo, A. V. Shevelkov, *J. Solid State Chem*. 2001, **161**, 233–242.
44 (a) J. V. Zaikina, K. A. Kovnir, U. Schwarz, H. Borrmann, A. V. Shevelkov, *Z. Kristallogr. NCS,* 2007, **222**, 177−179. (b) K. Kishimoto, T. Koyanagi, K. Akai, M. Matsuura, *Jap. J. Appl. Phys., Part 2*, 2007, **46,** L746−L748. (c) F. Philipp, P. Schmidt, *J. Cryst. Growth* 2008, **310**, 5402−5408. (d) J. V. Zaikina, K. A. Kovnir, U. Burkhardt, W. Schnelle, F. Haarmann, U. Schwarz, Yu. Grin, A. V. Shevelkov, *Inorg. Chem*. 2009, **48**, 3720−3730. (e) J. V. Zaikina, T. Mori, K. Kovnir, D. Teschner, A. Senyshyn, U. Schwarz, Yu. Grin, A. V. Shevelkov, *Chem. Eur. J*. 2010, **16**, 12582−12589.
45 (a) N. Jaussaud, M. Pouchard, G. Goglio, C. Cros, A. Ammar, F. Weill, P. Gravereau, Solid State Sci. 2003, **5**, 1193-1200. (b) N. Jaussaud, P. Toulemonde, M. Pouchard, A. San Miguel, P. Gravereau, S. Pechev, G. Goglio, C. Cros, *Solid State Sci*. 2004, **6**, 401−411. (c) N. Jaussaud, M. Pouchard, P. Gravereau, S. Pechev, G. Goglio, C. Cros, A. San Miguel, P. Toulemonde, *Inorg. Chem*. 2005, **44**, 2210−2214.
46 (a) K. Kishimoto, K. Akai, N. Muraoka, T. Koyanagi, M. Matsuura, *Appl. Phys. Lett*. **89**, 2006, 172106. (b) M. A. Kirsanova, L. N. Reshetova, A. V. Olenev, A. M. Abakumov, A. V. Shevelkov, *Chem. Eur. J.* 2011, **17**, 5719−5726.
47 M. A. Kirsanova, T. Mori, S. Maruyama, M. Matveeva, D. Batuk, A. M. Abakumov, A. V. Gerasimenko, A. V. Olenev, Yu. Grin, A. V. Shevelkov, *Inorg. Chem.* 2013, **52**, 577−588.
48 J. Dunner, A. Mewis, *Z. Anorg. Allg. Chem.* 1995, **621**, 191−196.
49 J. Fulmer, O. I. Lebedev, V. V. Roddatis, D. C. Kaseman, S. Sen, J. A. Dolyniuk, K. Lee, A. V. Olenev, K. Kovnir, *J. Am. Chem. Soc.* 2013, **135**, 12313−12323.
50 L. G. Akselrud, P. Yu. Zavalii, Yu. N. Grin, V. K. Pecharsky, B. Baumgartner, E. Wölfel, *Mater. Sci. Forum*, 1993, **133–136**, 335−342.
51 K. Brandenburg, Diamond 3.0, Crystal Impact GbR, Bonn, Germany, 1997−2004.
52 G. Kresse, J. Furthmuller, *Phys. Rev. B,* 1996, **54**, 11169–11186.
53 J. P. Perdew, K. Burke, M. Ernzerhof, *Phys. Rev. Lett*. 1996, **77**, 3865–3868.

Table 2. Selected bond distances and angles (Å, °) of $Rb_{7.50(1)}Tl_{0.50(1)}Ge_{46}$ and $K_{7.62(1)}Tl_{0.38(1)}Ge_{45.34(3)}$.

$Rb_{7.50(1)}Tl_{0.50(1)}Ge_{46}$							
Rb1—8Ge2	3.4360 (9)	Rb2—Ge3	4.162 (1)	Ge3—Ge1—Ge3	111.82 (4)	Ge2—Ge3—Ge2	105.59 (5)
Rb1—12Ge3	3.563 (1)	Ge1—Ge3	2.520 (1)	Ge3—Ge1—Ge3	108.31 (4)	Ge2—Ge3—Ge1	106.80 (4)
Rb2—12Ge3	3.6514 (8)	Ge2—Ge3	2.4902 (7)	Ge3—Ge2—Ge3	110.84 (5)	Ge2—Ge3—Ge3	106.13 (5)
Rb2—4Ge1	3.8239 (1)	Ge2—Ge2	2.495 (1)	Ge3—Ge2—Ge2	108.07 (5)	Ge1—Ge3—Ge3	124.09 (5)
Rb2—8Ge2	4.0222 (2)	Ge3—Ge3	2.584 (2)				
$K_{7.62(1)}Tl_{0.38(1)}Ge_{45.34(3)}$							
K1—6Ge4	3.357 (3)	K2—Ge4	3.983 (5)	Ge5—Ge6	2.589 (4)	Ge5—Ge4—Ge4	105.01 (14)
K1—2Ge3	3.521 (3)	K2—3Ge4	4.083 (5)	Ge5—Ge1—Ge5	108.48 (10)	Ge1—Ge5—Ge4	110.69 (13)
K1—6Ge6	3.571 (3)	K2—3Ge4	4.326 (5)	Ge5—Ge1—Ge5	109.31 (10)	Ge1—Ge5—Ge3	104.88 (13)
K1—6Ge5	3.636 (3)	K2—2Ge6	4.387 (5)	Ge5—Ge1—Ge5	110.64 (10)	Ge1—Ge5—Ge6	126.83 (14)
K2—2Ge5	3.359 (4)	Ge1—4Ge5	2.400 (3)	Ge6—Ge2—Ge6	108.46 (10)	Ge4—Ge5—Ge3	106.51 (14)
K2—2Ge6	3.460 (4)	Ge2—4Ge6	2.463 (3)	Ge6—Ge2—Ge6	111.52 (10)	Ge4—Ge5—Ge6	103.60 (14)
K2—2Ge3	3.604 (5)	Ge3—Ge3	2.237 (4)	Ge3—Ge3—Ge5	108.72 (2)	Ge3—Ge5—Ge6	102.67 (14)
K2—2Ge5	3.606 (4)	Ge3—3Ge5	2.580 (4)	Ge5—Ge3—Ge5	110.21 (15)	Ge4—Ge6—Ge2	103.40 (13)
K2—2Ge1	3.621 (3)	Ge4—Ge6	2.430 (4)	Ge6—Ge4—Ge5	115.68 (15)	Ge4—Ge6—Ge5	104.51 (14)
K2—2Ge5	3.889 (5)	Ge4—Ge5	2.495 (4)	Ge6—Ge4—Ge6	115.48 (15)	Ge2—Ge6—Ge4	112.57 (13)
K2—2Ge6	3.950 (4)	Ge4—Ge6	2.516 (4)	Ge6—Ge4—Ge4	114.77 (15)	Ge2—Ge6—Ge5	122.27 (14)
K2—2Ge2	3.981 (3)	Ge4—Ge4	2.600 (4)	Ge5—Ge4—Ge6	107.56 (14)	Ge4—Ge6—Ge5	110.91 (14)

$Rb_{7.50(1)}Tl_{0.50(1)}Ge_{46}$ and $K_{7.62(1)}Tl_{0.38(1)}Ge_{45.34(3)}$ are synthesized and characterized.